Rev.Adv.Mater.Sci. 25 (2010) 82-87

NANOCRYSTALLINE STRUCTURE FORMATION AND MAGNETIC HYSTERESIS PROPERTIES OF Y-Fe-Co-B ALLOYS

I.S. Tereshina[1,2], E.A. Tereshina[2,3], G.S. Burkhanov[1] and S.V. Dobatkin[1]

[1]Baikov Institute of Metallurgy and Material Science RAS, 119991 Moscow, Leninskii pr. 49, Russia
[2]International Laboratory of High Magnetic Fields and Low Temperatures, 95 Gajowicka str., 53-421 Wroclaw, Poland
[3]Institute of Physics, Academy of Sciences, Na Slovance 2, 18221 Prague, Czech Republic

Received: November 30, 2009

Abstract. In the present work a study of the influence of structural state on magnetic hysteresis properties of $Y_2(Fe_{1-x}Co_x)_{14}B$ compounds was carried out. Starting alloys were prepared by induction melting in an Ar atmosphere. Y-Fe-Co-B alloys with a nanograin structure were obtained by various techniques such as a severe plastic deformation (SPD) and by the classical melt spinning. Electron microscopy and X-ray analysis were used for the structural investigation. The magnetization measurements were performed using a SQUID magnetometer. It is shown that the relatively high values of coercive force are observed in such weakly-anisotropic alloys as $Y_2(Fe_{1-x}Co_x)_{14}B$ in case of achieved nanograin structure. The effect of remanence enhancement over than 0.5 is observed in rapidly quenched $Y_2Fe_{14}B$ alloys at T = 4.2K. The influence of hydrogen on magnetic hysteresis properties is studied as well.

1. INTRODUCTION

The existing international scientific and technical demand for the high-energy magnets stimulates an intensive search of new hard magnetic materials. The alloys containing the rare-earth and 3d transition metals are the most perspective materials for the permanent magnets production [1,2]. From the practical point of view, the main interest is pointed to the alloys containing iron as a 3d transition metal ($Nd_2Fe_{14}B$, $Sm_2Fe_{17}N_3$ *et al.*) [3]. During last two decades the development and rapid implementation of industrial production of bulk magnets on the base of Nd-Fe-B system resulted in both the considerable increase of production and diversification of the permanent magnet applications (in atomic and space technology, oil processing industry, *etc*.) [4,5].

As the development of nanotechnology progresses, perspectives of creation of nanostructured hard magnetic materials (NHMM) with characteristics exceeding those of bulk magnets gets opened up. In order to obtain NHMM, few methods such as rapid quenching, severe plastic deformation (SPD), adapted HDDR (processes named

Corresponding author: I.S. Tereshina, e-mail: teresh@imet.ac.ru

after the procedures of Hydrogenation, Disproportionation, Desorption and Recombination), methods of mechanical activation, mechanical alloying as well as various film technologies are used [6-11]. However, in spite of achieved success in optimization of the alloys compositions and improvement the methods mentioned above, a set of existing problems (low characteristics of derived materials, their heterogeneous structure and absence of the technology of obtaining the anisotropic (textured) nanocomposite magnets etc.) impedes the progress in realization of the full potential of NHMM.

It should be noted that among various NHMM, an investigation of the magnetic hysteresis properties of nanostructured materials of the $R_2Fe_{14}B$ type attracts much attention of scientists working in metallophysics and magnetism fields, due to the fact that the properties of NHMM differ much from those of polycrystalline materials [12,13]. It is known that the rapidly quenched Nd-Fe-B alloy [14-17] reveals the effect of the remanence enhancement (remanent magnetization σ_r exceeds that of the estimated theoretically value of 0.5 σ_s (saturation magnetization) for the ensemble of the single-domain, randomly oriented particles [18]). This phenomenon can be explained by the effect of exchange coupling between the grains of the nanostructured materials, which tends to orient their magnetization vectors despite the mismatch in the easy-axes orientations. If such a material contains the soft magnetic phase with a high saturation magnetization in addition to the hard one, then, due to exchange interaction, their magnetization will coincide with the magnetization of the hard magnetic phase. As a result, high values of remanence can be achieved in the isotropic magnet. This effect is known as the effect of remanence enhancement. On the other hand, the dependence of this phenomenon on the type of both R and 3d-ions and the magnetocrystalline anisotropy of such ionic subsystems was never studied systematically. Systematic data on the size and shape of the hard magnetic phase crystallites, presence and volume of the soft magnetic phase, and the influence of hydrogen on parameters of magnetic hysteresis (it is known that under normal conditions practically all rare earth intermetallics contain some quantity of hydrogen penetrated through the pores and microcracks) is missing as well.

The aim of the present work is to study systematically the effect of structural state on magnetic properties of $Y_2Fe_{14}B$ compound (Y is a nonmagnetic analog of REMs) with partial substitution of Co for Fe in order to reach deeper understanding of the 3d-sublattice magnetism of these compounds. The effect of interstitial hydrogen on magnetic hysteresis properties is also investigated.

2. EXPERIMENTAL

The compounds $Y_2(Fe_{1-x}Co_x)_{14}B$ ($0 \le x \le 1$) were prepared by induction melting of the elements with purity of at least 99.95 wt.% under an argon atmosphere. Details of the sample preparation can be found e.g. in Ref. 19. Y-Fe-Co-B alloys with nanograin structure were obtained by two methods. In the first one, the nanocrystalline structure was formed by severe plastic deformation. The second method included sample preparation by the classical melt spinning process. Intense plastic deformation was performed in a Bridgman anvil by means of torsion under high hydrostatic pressure of 4 GPa at room temperature with achieved true strain of ~6 (5 revolutions) on samples with initial sizes of 10 mm in diameter and 0.6 mm in height. The structure investigation was performed by means of transmission electron microcopy (JEM 100 CX microscope) and by X-ray diffraction.

In addition, the initial ingots were remolten in quartz ampoules with an orifice and subjected to spinning (rapid quenching) at various speeds of the cooling wheel, *Vs* = 10-40 m/s. As a result of the spinning procedure, the materials were obtained in a form of ribbon fragments with a length of about 10 mm, 2-5 mm wide, and 0.03 mm thick. Scanning electron microscopy (LEO 430i microscope) and X-ray analysis were employed for structural investigation. The interaction with hydrogen was studied under the pressure of up to 13 atm. In order to initiate the reaction, the sample was heated up to 250 °C. No incubation period was required to start the hydrogenation process, and the reaction has ended with formation of the $Y_2Fe_{14}BH_2$ hydride. Subsequent analysis of diffraction patters allowed the conclusion that no segregation release of Fe occurred at that temperature, and the only hydride phase was formed.

The magnetic properties of $Y_2(Fe_{1-x}Co_x)_{14}B$ compounds were investigated using a SQUID magnetometer at T = 4.2K. The magnetization of $Y_2Fe_{14}B$ quenched samples was measured in a superconducting solenoid by a compensation method.

3. RESULTS AND DISCUSSION

3.1. Bulk materials

The structure analysis performed by means of X–ray diffraction at room temperature has shown that

Table 1. The lattice parameters a and c, the unit cell volume V and the saturation magnetization of $Y_2(Fe_{1-x}Co_x)_{14}B$ compounds.

Compound	$Y_2(Fe_{1-x}Co_x)_{14}B$							
x	0	0.1	0.2	0.3	0.4	0.6	0.8	1.0
a (nm)	0.8757	0.8749	0.8729	0.8725	0.8720	0.8688	0.8628	0.8607
c (nm)	1.2040	1.199	1.197	1.196	1.195	1.188	1.184	1.1731
V (nm^3)	0.923	0.919	0.912	0.910	0.909	0.898	0.881	0.868
M_S (emu/g) (*T*=4.2K)	177	175	170	163	155	140	123	106

all $Y_2(Fe_{1-x}Co_x)_{14}B$ alloys contain practically only 2-14-1 phase with the lattice parameters as presented in Table 1. The content of impurity phases was negligibly small.

Fig. 1a shows the hysteresis loop of bulk $Y_2Fe_{14}B$ measured at *T* = 4.2K. The presented curves show no hysteresis. Similar situation is observed in $Y_2(Fe_{1-x}Co_x)_{14}B$ compounds. The data on saturation magnetization for $Y_2(Fe_{1-x}Co_x)_{14}B$ are also presented in Table 1. The obtained results agree well with literature [3,20]. As one can see from the Table 1, all the parameters (*a*, *c*, *V* and M_s) decrease monotonously as the Co concentration increases.

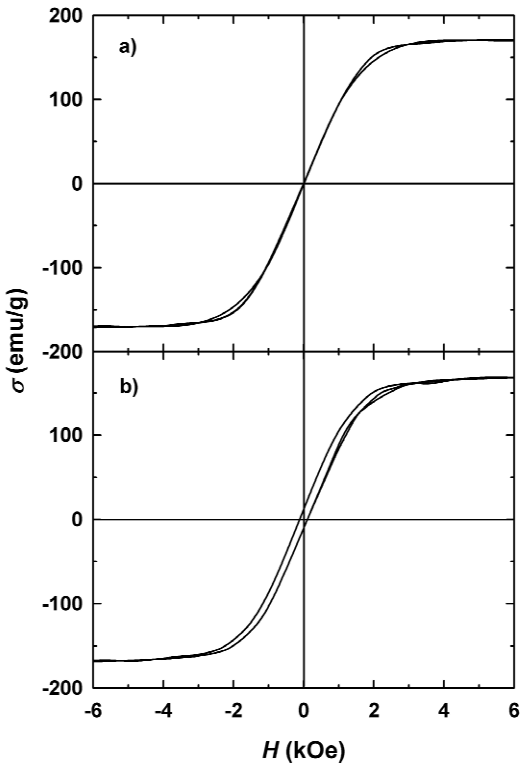

Fig. 1. Hysteresis loops measured at *T* = 4.2K for bulk (a) and nanocrystalline (b) $Y_2Fe_{14}B$.

3.2. Nanostructured $Y_2(Fe_{1-x}Co_x)_{14}B$ alloys obtained by SPD

Fig. 2 shows the TEM image of $Y_2Fe_{14}B$ alloy after SPD. The electron microscopy investigation have revealed presence of structural elements with the sizes of 250-450 nm, partly having the large-angle borders as it follows from the observed point reflections located circularly on the electron-diffraction pattern in Fig. 2a. Moreover, a substructure with small misorientation of the borders and the sizes of elements of 50-100 nm is observed within the structural elements described above (see Fig. 2b). In a dark field, an agglomeration of 5-10 nm size structure elements (second-phase particles, i.e. α-Fe) is seen.

The hysteresis loop measured at *T* = 4.2K for the nanostructured $Y_2Fe_{14}B$ is presented in Fig. 1b. Narrow hysteresis appeared in the sample after SPD processing shows that the value of coercive force has increased as compared to bulk $Y_2Fe_{14}B$ material (see Fig.1a). As it is seen from Fig. 3 (*a*, *b*, *c*

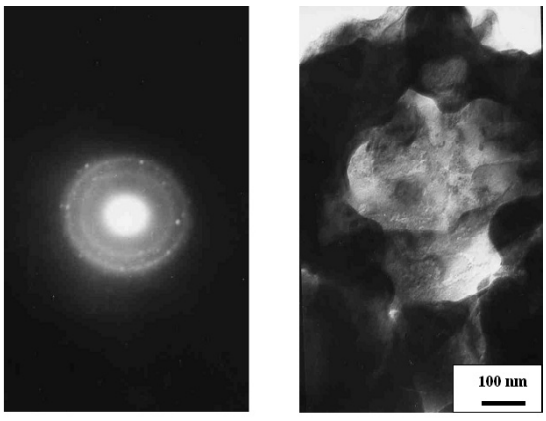

Fig. 2. TEM images of $Y_2Fe_{14}B$ alloy after SPD.

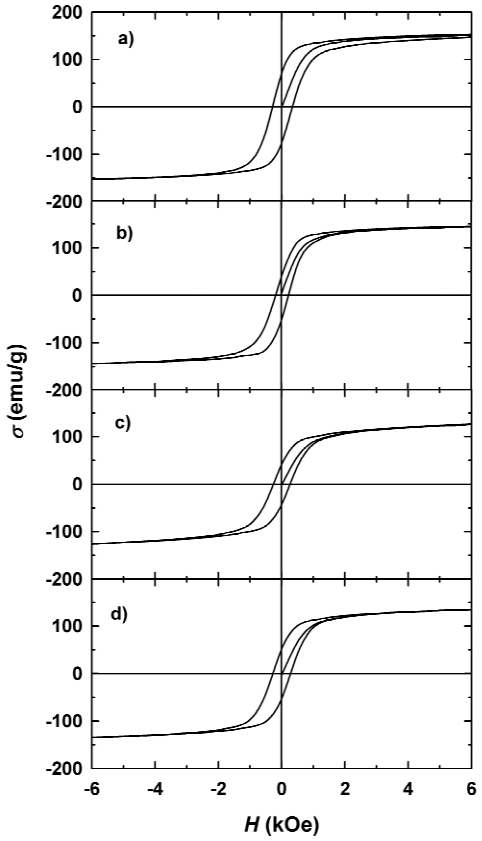

Fig. 3. Hysteresis loops for nanocrystalline $Y_2(Fe_{1-x}Co_x)_{14}B$ at T = 4.2K: x = 0.2 (a); 0.3 (b); 0.4 (c); 0.6 (d).

and *d*), a visible hysteresis is also observed in all the nanostructured $Y_2(Fe_{1-x}Co_x)_{14}B$ samples under study (we have investigated the samples with the uniaxial magnetic anisotropy is samples with Co concentration $0 \le x \le 6$). An analysis of the obtained curves shows that the dependence of coercivity on Co concentration demonstrates non-monotonous behavior (see Fig. 4). The maximum of coercivity (~300 Oe) is found in the $Y_2(Fe_{0.8}Co_{0.2})_{14}B$ alloy with the relation $\sigma_r/\sigma_s = 0.45$. Therefore, we may conclude that the resultant microstructure in the obtained samples doesn't allow to form the high-coercivity state and to observe the effect of the remanence enhancement. Nevertheless, and on our opinion, it is possible to obtain nanostructured samples similar to those rapidly-quenched $Y_2Fe_{14}B$ (see below) with achieved high values of coercive force and high remanence by changing the technological parameters and using thermal treatment procedures.

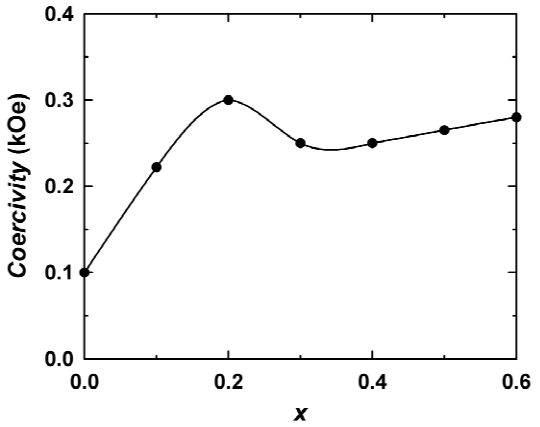

Fig. 4. Concentration dependence of coercivity for nanocrystalline $Y_2(Fe_{1-x}Co_x)_{14}B$ at T = 4.2K.

3.3. Nanostructured $Y_2Fe_{14}B$ alloys produced by melt spinning and their hydrides

Samples of $Y_2Fe_{14}B$ alloy were obtained at speeds V_s = 20, 30, and 40 m/s of the quenching wheel. As it follows from the X-ray diffraction data, the main phase crystallizes in the tetragonal $Nd_2Fe_{14}B$-type structure with a content of α-Fe impurity of 5-6%. The lattice parameters and the unit cell volume of the main phase were found to grow with the increase of the quenching rate.

The spinning of $Y_2Fe_{14}B$ did not induce the amorphous phase. A strong decrease of reflection intensities with the increase of cooling wheel speed was observed, whereas the reflections widths kept constant. We denoted a state of quenched $Y_2Fe_{14}B$ samples as defective one. In order to obtain information about the defective phase content, the neutron reflection (101) was measured for the crystalline and $Y_2Fe_{14}B$ samples quenched at various V_s [21]. Intensities were reduced to the same sample mass, exposition time and corrected for the absorption coefficient. This procedure allowed us to estimate the quantities of the defective phase, which were equal to 10±5, 37±10 and 75±10% for the samples with V_s = 20, 30, and 40 m/s, respectively. The particle sizes determined by the small-angle neutron scattering method (SANS) were found to equal to 100, 40, and 40 nm for the samples quenched under V_s = 20, 30, and 40 m/s, respectively. Non-uniform distributions of larger grains (clusters of several crystallites) were observed by scanning electron microscopy.

Both microstructure and magnetic properties of the rapidly-quenched ribbons of Y-Fe-B alloys are extremely sensitive to the change of the quenching speed. Measurements of magnetic hysteresis loops $\sigma(H)$ of quenched samples were performed at 4.2K (see Fig. 5). It was found that the samples behave as soft magnetic materials with negligible coercive force after processing at the quenching speed of 40 m/s. The largest coercive force values were observed for the sample obtained at 30 m/s, e.g. ${}_iH_c$ = 1.0 kOe and 1.5. kOe at 4.2 and 300K, respectively. This quenching speed was found to be optimal. The lower quenching speed (20 m/s) leads to formation of the coarse-grained structure and, as the result, to the observed low coercive force. It is worth noticing that the effect of remanence enhancement in the isotropic uniaxial magnetic material above the level of 0.5 (σ_r/σ_s=0.55 at 4.2K) was observed in the sample obtained at 30 m/s speed. This ratio was found to decrease down to 0.45 at room temperature in spite of the coercive force increase.

Our investigation have shown that hydrogenation leads both to the increase of magnetization and to considerable change of hysteresis properties, namely, to the decrease of coercivity and remanence magnetization. Fig. 6 displays the hysteresis loops measured at T=4.2K for $Y_2Fe_{14}BH_y$ (quenched at 30 m/s). The change of magnetic hysteresis properties in $Y_2Fe_{14}BH_2$ as compared to the parent compound can be caused by two reasons. As the first one, an increase of the grains (for 2.5-3 times on the average) of the 2-14-1 phase as a result of the heating of the sample during the hydrogenation procedure can be named. The second reason (and the main one) is the decrease of energy of magnetocrystalline anisotropy (decrease of the anisotropy field of the 2-14-1 phase) as a result of hydrogenation.

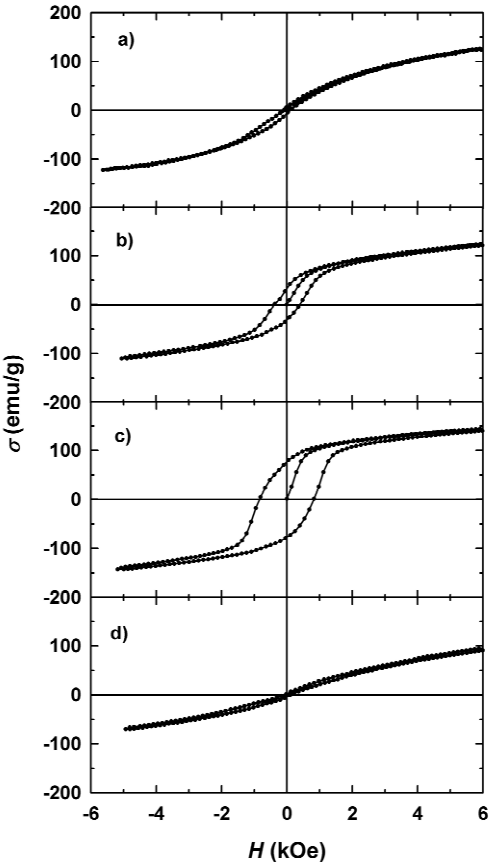

Fig. 5. Hysteresis loops measured at T=4.2K for bulk (a) and quenched at Vs=20 (b), 30 (c), and 40 (d) samples of $Y_2Fe_{14}B$ alloys.

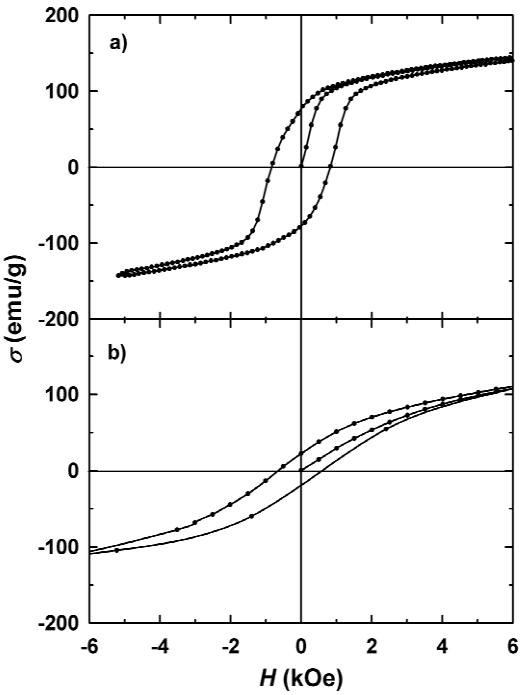

Fig. 6. Hysteresis loops measured at T=4.2K for $Y_2Fe_{14}BH_y$ quenched at 30 m/s: y = 0 (a) and y = 2 (b).

4. CONCLUSIONS

Complex investigation of the structure and magnetic hysteresis properties of nanostructured hard magnetic materials $Y_2(Fe_{1-x}Co_x)_{14}B$ was performed. Alloys with nanograin structure were obtained by two techniques such as a severe plastic deformation and classical melt spinning. Achievement of nanocrystalline state in $Y_2Fe_{14}B$ (Y is nonmagnetic ion) using the melt spinning technique (at the cooling wheel speed Vs = 30 m/s) has let to observe the effect of exchange enhancement of the remanence (σ_r/σ_s=0.55 at 4.2K) in the isotropic material. The structural peaks of the quenched $Y_2Fe_{14}B$ alloys were not broadened (and therefore, we call the

formed phase as defective, rather than amorphous). One can assume an existence of strong atomic displacements as possible reason of the appearance of the observed state.

It is found that hydrogen incorporation in the nanostructured materials leads to considerable decrease of both the coercive force and remanence. Nanocrystalline hard magnetic materials $Y_2(Fe_{1-x}Co_x)_{14}B$ obtained by severe plastic deformation may also reveal hysteresis properties, although in order to obtain high values of magnetic characteristics, the conditions of sample preparation should be worked out. The conducted research may help to obtain better insight into the magnetism of 3d transition metal sublattice (in particular the effect of structural state on magnetic hysteresis properties) in such an important class of magnetic materials as $R_2(Fe,T)_{14}B$.

The work has been supported by RFBR, pr. №09-03-12103 and №10-03-00848.

REFERENCES

[1] J.M.D. Coey, *Rare-earth Iron Permanent Magnets* (Clarendon Press, Oxford, 1996).

[2] H. Kronmuller, In: *Supermagnets, Hard Magnetic Materials*, ed. by G.J. Long and F. Grandjean (Kluwer: Dordrecht, 1991) p.461.

[3] J.F. Herbst // *Review of Modern Physics* **63** (1991) 819.

[4] V. Panchanathan, *Proc. 16th Int. Symp. on Magn. Anizotropy and Coercivity in RE-TM alloys* (Sendai, 2000) p.431.

[5] J.M.D. Coey // *J. Magn.Magn.Mater*. **248** (2002) 441.

[6] J.J. Croat, J.F. Herbst, R.W. Lee and F.E. Pinkerton // *J. Appl. Phys.* **55** (1984) 2078.

[7] L.I. Gang, *Proc. 19th Int. Workshop on REPM and their applications* (Beijing, 2006) p.316.

[8] N.M. Dempsey, A. Walther, F. May, D. Givord, K. Khlopkov and O. Gutfleisch // *Appl. Phys. Lett.* **90** (2007) 092509.

[9] Yu.D. Yagodkin, A.S. Lileev, J.V. Lyubina, E.N. Shingarev, V.A. Glebov and V.S. Nefedov // *J. Magn.Magn.Mater*. **258-259** (2003) 586.

[10] O. Gutfleisch and I.R. Harris // *J. Phys*. **29** (1996) 2255.

[11] L. Schultz, J. Wecker and E.J. Hellstern // *J. Appl. Phys*. **61** (1987) 3583.

[12] J. Bernardi, J. Figler, M. Sagawa and Y. Hirose // *J. Appl. Phys*. **83** (1998) 6396.

[13] Z.Q. Jin, H. Okumura, H.L. Wang, J.S. Munoz, V. Papaefthymiou and G.C. Hadjipanayis // *J. Magn.Magn.Mater.* **242-245** (2002) 1307.

[14] J. Bauer, M. Seeger, A. Zern and H. Kronmuller // *J. Appl. Phys.* **80** (1996) 1667.

[15] R. Coehoorn, D.B. de Mooji, J.P.W. Duchateau and K.H.J. Buschow // *J. Phys.* **49** (1988) C8-669.

[16] G.B. Clemente, J.E. Keem and J.P. Bradley // *J. Appl. Phys.* **64** (1988) 5299.

[17] F. Matsumoto, H. Sakamoto, M. Komiya and M. Fujikura // *J. Appl. Phys*. **63** (1988) 3507.

[18] E.C. Stoner and E.P. Wohlfarth // *Philos. Trans. R. Soc.* **240** (1948) 599.

[19] N.V. Kudrevatykh, S.A. Andreev, M.I. Bartashevich, A.N. Bogatkin, O.A. Milyaev, P.E. Markin, I.S. Tereshina, T. Palewski and E.A. Tereshina // *J. Magn.Magn.Mater.* **300** (2006) E448.

[20] N.M. Hong, J.M. Franse and N.P. Thuy // *J. Less-Com. Met*. **155** (1989) 151.

[21] S.G. Bogdanov, A.N. Pirogov, Yu.N. Skryabin, A.E. Teplykh, N.V. Kudrevatykh, P.E. Markin, I.S. Tereshina and T. Palewski, In: *Proceeding of "Moscow International Symposium on Magnetism (*MISM,2005), p. 189.